

## Reemitted-positron spectroscopy of cobalt and nickel silicide films

B. D. Wissman, D. W. Gidley, and W. E. Frieze

*Department of Physics, University of Michigan, Ann Arbor, Michigan 48109*

(Received 23 March 1992)

Reemitted-positron spectroscopy (RPS) has been employed in a systematic investigation of the positronic properties of the various phases ( $M_2Si$ ,  $MSi$ , and  $MSi_2$ ) of Co and Ni silicide films grown *in situ* on Si substrates. The positron work function  $\phi^+$  is found to be negative for all of the different phases, with the parameter  $\Sigma \equiv \mu^- + \mu^+$  having a surprisingly large variation. In an attempt to calibrate the size of shifts in  $\Sigma$  due to strained pseudomorphic growth of thin  $CoSi_2$  films, the positron deformation potential  $E_d^+ \equiv V(\partial\Sigma/\partial V)$  was determined using the thermal-expansion technique. However, pseudomorphic shifts for films of thickness less than 40 Å were found to be unobservable due to incomplete positron thermalization in such thin films. The deformation potential can also be used to estimate the size of the positron diffusion constant, which is found to be comparable to that of other metals. Thus the short positron diffusion length (of order 150 Å) determined from depth-profiling measurements of  $CoSi_2$  films must be a result of positron trapping in either the film or at the interface with the Si substrate. RPS results considered as a function of film thickness support the conclusion that defects in the film (misfit dislocations and/or vacancies) represent the major source of positron trapping.

### I. INTRODUCTION

There is a great deal of interest in the formation of metal silicide films due to their many device applications, such as Schottky barriers, Ohmic contacts, low-resistivity interconnects, and metal base and permeable base transistors.<sup>1-3</sup> A number of the metal silicides are known to grow epitaxially, and of these,  $CoSi_2$  and  $NiSi_2$  are of particular interest due to their small lattice mismatches with Si (1.2% and 0.4%, respectively<sup>4</sup>). These small lattice mismatches permit the growth of silicide films with nearly perfect epitaxial structure on Si substrates, which, under certain conditions, may be pseudomorphic.<sup>1,5,6</sup>  $CoSi_2$  has been discussed as a candidate material for the fabrication of a metal base transistor due to its low-resistivity, long electron mean free path, and the fact that Si may be epitaxially grown over epitaxial  $CoSi_2$  films.<sup>1,2</sup> In addition to their technological applications, the possibility of growing silicide films which have nearly perfect interfaces with Si substrates makes them ideal systems in which to study the basic physics of metal-semiconductor junctions.<sup>4</sup>

Early interest in positron reemission studies of silicides was motivated by the prospect of exploiting the large mobility of positrons in Si to construct a more efficient moderator for slow positron beams. One would like to apply a large electric field to drift the implanted positrons to the surface.<sup>7</sup> Such a field-assisted moderator requires an electrical contact which has an appropriate positron energy level so that the diffusing positrons do not encounter an energy barrier at the interface. Moreover, the contact should be epitaxially grown to minimize defects which may trap the positrons;<sup>7,8</sup> hence  $CoSi_2$  was suggested as a candidate material.<sup>8</sup> Such metal silicides that are epitaxially grown on a Si substrate are also attractive systems for studying the diffusion, drift,<sup>9</sup> and trapping of positrons in the vicinity of the Schottky *well* and the as-

sociated depletion region. However, very little is known about the properties that determine positron transport in these materials. The only study<sup>10</sup> is of  $CoSi_2$ , in which it was discovered that a thin film grown on a Si(111) substrate has a negative positron work function,  $\phi^+$ .  $CoSi_2$  therefore reemits positrons; thus the techniques of reemitted-positron spectroscopy (RPS) can be applied to this and other silicide systems.

In RPS one measures the energy distribution of positrons which are reemitted after being implanted with incident energies of order several keV, thermalizing, and subsequently diffusing back to the surface. The energy spectrum of positrons reemitted from a well-ordered surface with a negative  $\phi^+$  typically has a narrow peak, corresponding to positrons emitted elastically with kinetic energy equal to  $|\phi^+|$ . Due to the presence of contact potentials, the energy of positrons emitted in the elastic peak is determined<sup>11</sup> by a parameter  $\Sigma$ , where

$$\Sigma \equiv \mu^- + \mu^+ = -(\phi^- + \phi^+) . \quad (1)$$

Here  $\mu^-$  and  $\mu^+$  are the *bulk* electron and positron chemical potentials, and  $\phi^-$  and  $\phi^+$  are the electron and positron work functions, respectively. Note that  $\Sigma$  (referred to as the *positron affinity* in Ref. 12) is negative, and that a more negative value indicates a stronger affinity of a particular material for positrons.<sup>12</sup> A tail of inelastically scattered positrons extends down in energy to the zero energy cutoff, which is determined by  $\phi^-$ . There can also be a tail at energies  $> |\phi^+|$  due to "non-thermals" (i.e., positrons which failed to fully thermalize before being reemitted).

RPS has been shown to be a useful probe of multilayer systems.<sup>11,13,14</sup> In a metallic multilayer structure, each layer possesses a unique value of  $\Sigma$ . Since it is determined solely by bulk properties,  $\Sigma$  is independent of the presence of any overlayers or surface contamination. Thus positrons which have been implanted into a multi-

layer structure may be reemitted with well-defined energies which are characteristic of each material. By identifying the peak energy and any shifts thereof, RPS can be used to probe heterogeneous growth systems, e.g., interdiffusion alloying<sup>11</sup> and pseudomorphism.<sup>13</sup> In particular, in the present work we can observe the thermal reaction of metal layers deposited on Si to form the various silicides.

In this paper we report the results of a systematic RPS study of the various phases ( $M_2Si$ ,  $MSi$ , and  $MSi_2$ ) of Co and Ni silicide films grown *in situ* on Si substrates. RPS spectra are investigated as a function of the initial thickness of the metal overlayer, the annealing temperature, the incident positron energy, and the orientation of the Si substrate. The Si substrates have positive  $\phi^+$ , and the observed weak reemission is attributed to positrons which failed to fully thermalize in the crystal. In the case of the silicides,  $\phi^+$  is found to be negative for all of the different phases.  $\Sigma$  has a surprisingly large variation with stoichiometry, thus allowing each phase to be clearly distinguished in the RPS spectrum. We also determine  $\phi^-$  for each silicide relative to that of a Ni(100) reference crystal. All of the silicides are found to have a relatively low yield of reemitted positrons. This is attributed to a very short positron diffusion length, which is due to a high density of misfit dislocations and/or vacancies which are trapping the positrons. In an attempt to observe and calibrate shifts in  $\Sigma$  due to strained pseudomorphic growth of thin  $CoSi_2$  films, the positron deformation potential,  $E_d^+ \equiv V(\partial\Sigma/\partial V)$ , is determined using the thermal-expansion technique.

## II. EXPERIMENTAL TECHNIQUE

Co and Ni silicides were grown *in situ* by thermal reaction of thin (5–200 Å) Co and Ni films which had been deposited by evaporation from a heated W filament onto Si substrates which were at room temperature. All work was performed in an ultrahigh-vacuum (UHV) surface-analysis chamber, with base pressure  $1 \times 10^{-10}$  Torr. The background pressure in the chamber remained below  $2 \times 10^{-7}$  Torr at all times during the deposition and annealing. Silicide growth was monitored by both Auger electron spectroscopy (AES) and low-energy electron diffraction (LEED), with the various silicide phases obtained by varying the annealing time and temperature.<sup>15</sup> Co film thicknesses were determined by a quartz thin-film monitor, while Ni film thicknesses were estimated using AES. The Si substrates used were single crystals of either (100) or (111) orientation, with various doping levels (both *n* and *p* type,  $\rho = 0.1$ –3000  $\Omega$  cm). Annealing was accomplished by electron-beam heating of the samples, with the temperature monitored by a thermocouple. The substrates were cleaned by sputtering with 1–2-keV Ar ions, followed by a quick (<30-s) heat to 1100–1200 °C. Samples cleaned in this manner exhibited good LEED patterns, and had negligible surface contaminations of C (as determined by AES). In the case of the (111) substrates, the  $7 \times 7$  surface reconstruction was typically observed.

RPS studies were done using a variable-energy (0.5–4.0-keV) monoenergetic beam, providing on the or-

der of  $10^4$  positrons per second on the sample. At these beam energies the mean implantation depth<sup>16</sup>  $\bar{z}$  varies from approximately 25–750 Å. Unless otherwise stated, all spectra presented in the following sections were acquired with positrons of 1.0-keV incident energy. The energies of the reemitted positrons were measured with a double-pass cylindrical mirror analyzer operating in a constant pass-energy mode.<sup>11</sup> The value of  $\Sigma$  is determined by the energy of the elastic peak relative to that of a Ni(100) reference crystal, with  $\Sigma_{Ni}$  taken to be  $-3.8$  eV, as discussed below. The absolute-energy scale is calibrated by defining  $\phi^-$  (and hence the zero positron energy cutoff) of the clean Ni(100) crystal to be 5.2 eV.<sup>17</sup>  $|\phi^+|$  is determined by the energy difference between the elastic peak and the corresponding zero energy cutoff, minus a correction due to the resolution of the analyzer. The effect of the analyzer's finite energy resolution is to shift the apparent cutoff toward lower positron energies, resulting in an overestimation of  $|\phi^+|$ . The exact size of this resolution shift is difficult to determine, as it depends upon a convolution of the tails of the analyzer's energy-resolution function with the inelastic positron spectrum, which are not well known. Thus on an absolute scale our measurements of  $\phi^+$  and  $\Sigma$  are uncertain at the  $\pm 0.1$ -eV level. However, by measuring  $\Sigma$  relative to a reference crystal, the relative values of  $\Sigma$  can be determined to an accuracy of approximately  $\pm 20$  meV.  $\phi^-$  is determined relative to that of the Ni reference crystal by comparing the respective zero energy cutoffs. The measurement of  $\phi^-$  is largely unaffected by the resolution shift, as its size is approximately the same for both the sample and the reference crystal. Thus, relative values of  $\phi^-$  may be determined to an accuracy of approximately  $\pm 50$  meV. The clean Ni(100) reference crystal is found (after a resolution-shift correction of 0.25 eV) to have  $\phi^+ = -1.4$  eV, therefore from Eq. (1)  $\Sigma_{Ni} = -3.8$  eV.

## III. RPS OF Si SUBSTRATE

In the case of Si  $\phi^+$  is *positive*, thus the elastic emission of thermalized positrons is energetically forbidden. A low rate of positron reemission (of order 1% of that of a Ni single crystal) is observed; this is interpreted as being due to the nonthermal tail of the positron energy distribution. This tail may be well populated as the band gap of Si leads to a reduced efficiency of energy-loss processes for positrons with energy of order several eV. This interpretation is also consistent with the large negative value of  $\Sigma = -6.95$  eV predicted<sup>12</sup> for Si, and hence a correspondingly large and positive  $\phi^+$ . Further support for this conclusion is provided by the results of our RPS studies of oxide layers grown on Si single crystals. Figure 1 shows spectra acquired with positrons of incident energy 1 keV ( $\bar{z} \approx 175$  Å) for *n*-Si(100) ( $\rho \approx 0.01$   $\Omega$  cm) before and after thermal desorption of the native oxide layer. The spectra are similar in shape, but the total (energy-integrated) yield of reemitted positrons from the oxidized Si is a factor of 2 higher than that of the clean surface. The increased total yield is consistent with a simple shift in the zero energy cutoff due to the increase in  $\phi^-$ . This shift makes the emission of more, lower energy, non-

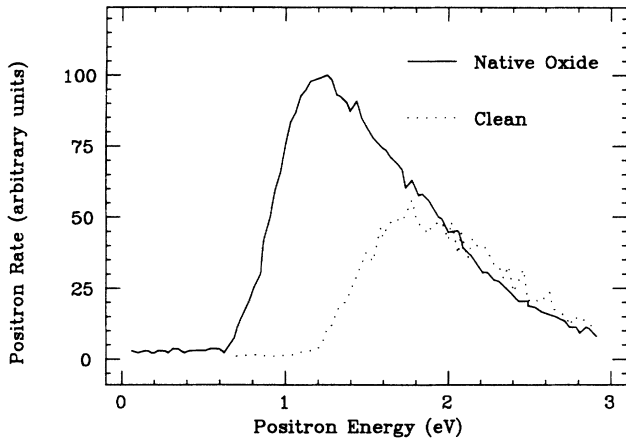


FIG. 1. RPS spectra, acquired at RT using 1-keV positrons, of Si(100) before and after thermal desorption of the native oxide layer. Note the shift in the zero energy cutoff, and the corresponding increase in reemission due to the presence of the oxide.

thermal positrons energetically possible. Despite the fact that the cutoff is shifted approximately 0.5 eV, thermalized positron emission is still not observed, thus indicating that for clean Si  $\phi^+ > 0.5$  eV. Furthermore, when the incident-beam energy is increased to 4 keV ( $\bar{z} \approx 1600$  Å) the total positron yield from the clean Si surface drops further by a factor of 6, indicative of much fewer non-thermals diffusing back to the surface. Similar results were obtained for oxide layers grown *in situ* on a variety of Si substrates.

#### IV. RPS OF SILICIDES

##### A. Co silicides on Si(111)

A Co film of thickness 100 Å was deposited on an *n*-Si(111) substrate ( $\rho \approx 0.13$  Ω cm) and annealed at progressively higher temperatures to produce the different silicide phases: Co<sub>2</sub>Si, CoSi, and CoSi<sub>2</sub>, in order of increasing reaction temperature. Assuming uniform layer growth, this amount of Co would produce silicide film thicknesses of approximately 150, 200, and 350 Å, respectively.<sup>18</sup> The corresponding mean implantation depths for 1-keV positrons range from approximately 50–80 Å. Several of the RPS spectra for Co-rich films (low reaction temperatures) are shown in Fig. 2. At annealing temperatures below 300 °C the RPS spectrum indicated the presence of only unreacted Co, consistent with AES. After annealing for 5 min at 300 °C, the RPS spectrum had distinct Co and Co<sub>2</sub>Si peaks, plus a mound at the energy corresponding to CoSi. An isolated Co<sub>2</sub>Si peak was never seen—it was always accompanied by Co and CoSi peaks. This was also the case for silicide films grown from Co films of initial thicknesses of 150 and 200 Å, consistent with the observation that the growth of Co<sub>2</sub>Si and CoSi occurs simultaneously.<sup>19,20</sup> Further annealing at 300 °C resulted in a transition from Co<sub>2</sub>Si to CoSi, with the size of the CoSi peak increasing relative to that of Co<sub>2</sub>Si with

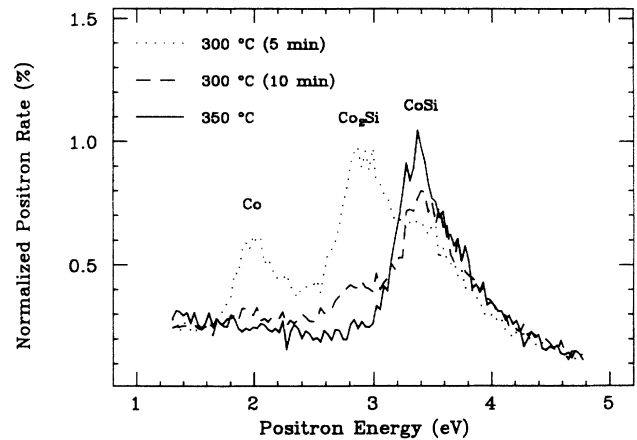


FIG. 2. RPS spectra, acquired at RT using 1-keV positrons, showing the progression from unreacted Co (as deposited at RT), to Co<sub>2</sub>Si, to CoSi with increased annealing time and temperature for a Co film of thickness 100 Å deposited on a Si(111) substrate. The spectra are normalized such that the vertical scale represents the peak rate as a percentage of that of the Ni(100) reference crystal. The zero of the energy scale corresponds to  $|\Sigma| = 5.2$  eV (thus the Ni peak would be at 1.4 eV).

increasing annealing time. After annealing for 10 min at 350 °C the Co<sub>2</sub>Si peak disappeared, leaving a lone CoSi peak. The transition from CoSi to CoSi<sub>2</sub> occurred after annealing near 450 °C. At reaction temperatures above 550 °C, a lone peak corresponding to CoSi<sub>2</sub> was observed, with LEED indicating a highly ordered surface. The RPS spectrum of a Co film of thickness 200 Å which was annealed at 850 °C to form CoSi<sub>2</sub> is shown in Fig. 3, plotted on a logarithmic scale. Clearly evident is the tail of inelastically emitted positrons, which extends down 0.85

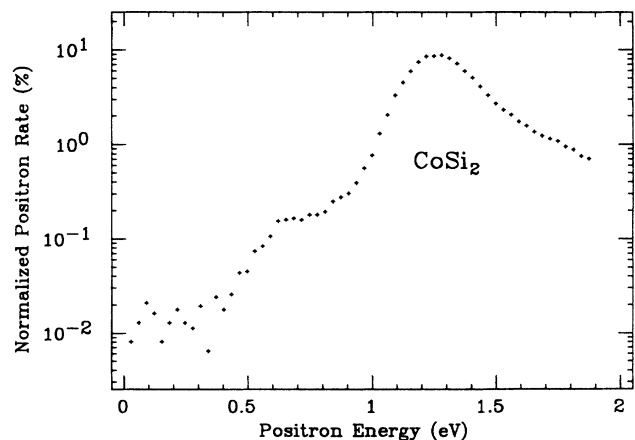


FIG. 3. RPS spectrum, acquired at RT using 1-keV positrons, of a CoSi<sub>2</sub> film approximately 700 Å thick, plotted on a logarithmic scale. Note the tail of inelastically emitted positrons extending down in energy to the zero cutoff. The film was grown by depositing 200 Å of Co on a Si(111) substrate and annealing at 850 °C. The spectrum is normalized and scaled as per Fig. 2.

eV from the peak to the zero energy cutoff. After correction for the 0.25-eV resolution shift,  $\phi^+$  is therefore  $-0.60 \pm 0.05$  eV.

### B. Ni silicides on Si(111)

A Ni film of thickness approximately 50 Å was deposited on a *p*-Si(111) substrate ( $\rho \approx 3000 \Omega \text{ cm}$ ) and annealed at progressively higher temperatures to produce the different silicide phases: Ni<sub>2</sub>Si, NiSi, and NiSi<sub>2</sub>, in order of increasing reaction temperature. Assuming uniform layer growth, this amount of Ni would produce silicide film thicknesses of approximately 75, 100, and 175 Å, respectively.<sup>18</sup> The corresponding mean implantation depths for 1-keV positrons range from approximately 50–80 Å. At annealing temperatures below 250°C the RPS spectrum indicated the presence of only unreacted Ni, consistent with AES. A distinct NiSi peak appeared in the RPS spectrum after annealing at 250°C. The Ni<sub>2</sub>Si phase was not observed with either AES or RPS. This may be explained by the relatively small growth rate at low temperature of Ni<sub>2</sub>Si on substrates with (111) orientation.<sup>15</sup> Thus in order to grow the metal-rich phase one has to anneal at temperatures below 250°C for very long times. At or above this temperature the growth of the intermediate phase proceeds rapidly, with the consumption of the metal-rich phase. The transition from NiSi to NiSi<sub>2</sub> occurred after annealing near 550°C, with the size of the NiSi<sub>2</sub> peak increasing relative to that of NiSi with increasing annealing time and temperature. At reaction temperatures above approximately 750°C, a lone peak corresponding to NiSi<sub>2</sub> was observed, with LEED indicating a highly ordered surface.

### C. Ni silicides on Si(100)

A Ni film of thickness approximately 50 Å was deposited on an *n*-Si(100) substrate ( $\rho \approx 10 \Omega \text{ cm}$ ) and annealed at progressively higher temperatures as shown in Fig. 4. A distinct Ni<sub>2</sub>Si peak appeared after annealing at 175°C, contrary to our previous results for a Si(111) substrate, in which Ni<sub>2</sub>Si was never observed. This is consistent with the enhanced growth rate of Ni<sub>2</sub>Si on (100)-oriented substrates compared to those with (111) orientation.<sup>15</sup> After annealing at 250°C a distinct NiSi peak appeared, consistent with the results from the (111) substrate. The transition to NiSi<sub>2</sub> began after reaction at 650°C, with LEED indicating a highly ordered surface. After annealing at 850°C a well-isolated peak corresponding to NiSi<sub>2</sub> was observed. All three Ni silicide phases are clearly distinguishable in Fig. 4, and it is interesting to note that their peaks are equal or higher in energy than that of pure Ni (i.e., despite the fact that  $\Sigma_{\text{Si}}$  has a low value the Ni silicides all have  $\Sigma \geq \Sigma_{\text{Ni}}$ ).

By increasing the incident positron-beam energy, and hence the mean implantation depth, we can sample progressively deeper below the surface. This simple form of depth profiling was used to demonstrate the transition from a NiSi film of thickness approximately 100 Å to a NiSi<sub>2</sub> film of thickness approximately 175 Å as the annealing temperature was increased from 650°C (Fig. 5) to

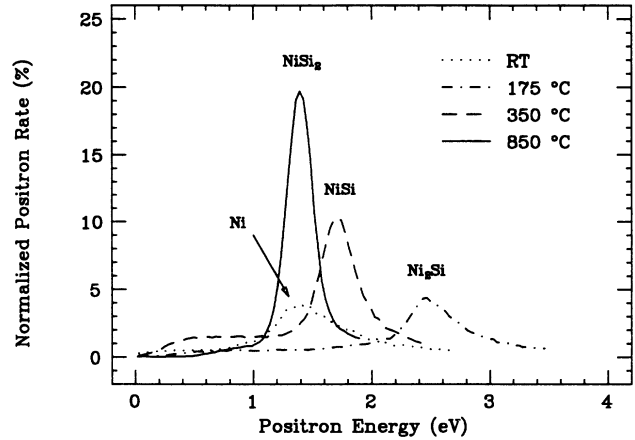


FIG. 4. RPS spectra, acquired at RT using 1-keV positrons, showing the progression from unreacted Ni (as deposited at RT), to Ni<sub>2</sub>Si, to NiSi, to NiSi<sub>2</sub> with increased annealing temperature for a Ni film of thickness approximately 50 Å deposited on a Si(100) substrate. The spectra are normalized and scaled as per Fig. 2.

750°C (Fig. 6). As can be seen in Fig. 5, the slightest hint of NiSi<sub>2</sub> is observed for the lowest implantation energy ( $\bar{z} \approx 25$  Å), indicating the presence of NiSi<sub>2</sub> near the surface, consistent with AES and LEED observations. After annealing at 750°C, the 4-keV spectrum ( $\bar{z} \approx 75$  Å) shows a NiSi peak, but the spectrum acquired using less penetrating 1-keV incident positrons ( $\bar{z} \approx 75$  Å) shows only a slight mounding at that energy, indicating the presence of deep-lying NiSi. These results are consistent with the motion of Ni atoms toward the NiSi/Si interface, resulting in the growth of NiSi<sub>2</sub> near the surface.

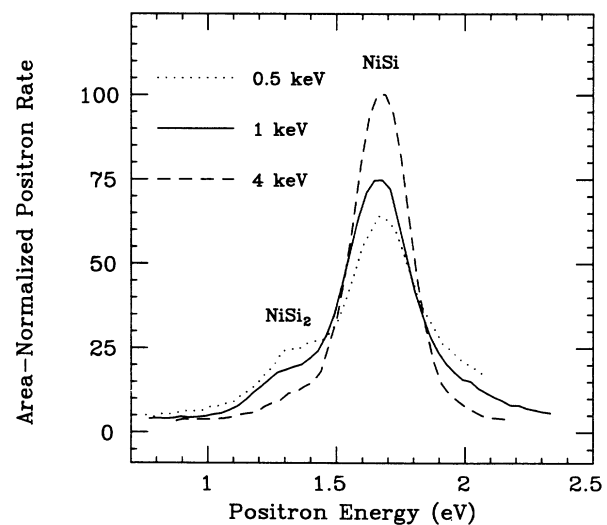


FIG. 5. RPS spectra, acquired at RT, of a Ni film of thickness approximately 50 Å deposited on a Si(100) substrate and annealed at 650°C, as a function of incident-beam energy. The spectra are normalized to equal areas. The zero of the energy scale corresponds to  $|\Sigma| = 5.2$  eV.

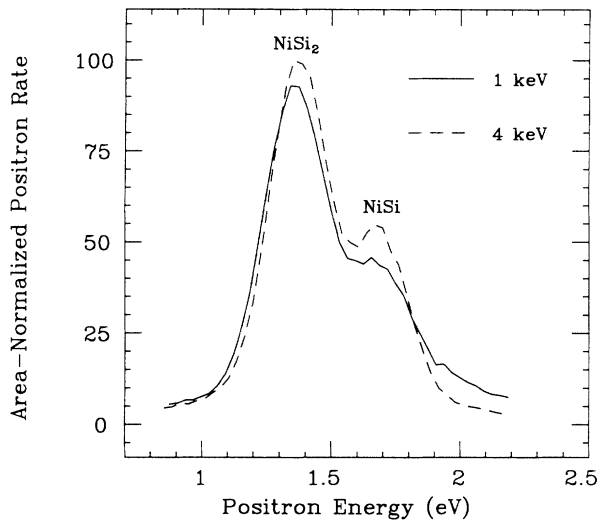


FIG. 6. RPS spectra, acquired at RT, as a function of incident-beam energy for the same film depicted in Fig. 5, now annealed at 750°C.

Indeed, implanted Xe marker experiments indicate that NiSi<sub>2</sub> is formed through the motion of Ni atoms away from the surface toward the Si substrate.<sup>21</sup> However, our results are not inconsistent with the proposed model,<sup>22</sup> in which growth of the NiSi<sub>2</sub> phase occurs by nucleation at the NiSi/Si interface, with subsequent growth normal to the interface, followed by lateral growth of the resulting columnar regions of NiSi<sub>2</sub>. Positrons which have thermalized in NiSi<sub>2</sub> would be prevented from entering NiSi by a 0.3-eV energy barrier, due to the higher  $\Sigma$  value of NiSi. Thus the reemission of positrons from deeplying NiSi<sub>2</sub> would be blocked by any overlying NiSi. Nevertheless, the film annealed at 750°C, in which the transformation from NiSi to NiSi<sub>2</sub> is nearly complete, has some remaining NiSi which is well below the surface, thus indicating that the final transformation occurs deep in the film.

#### D. Discussion of results

The results of the above spectra are summarized in Table I, and presented graphically in Fig. 7. All of the different silicides are found to have negative  $\phi^+$ . In all cases the  $\Sigma$  values are large enough that the silicide films present an energy barrier of several electron volts to positrons which have thermalized in the Si substrate (and thus would not be appropriate as electrical contacts for a field-assisted positron moderator). Of course, if the predicted<sup>12</sup> value of  $\Sigma_{\text{Si}}$  shown in Fig. 7 is correct, then it is very unlikely that any metal contact would be suitable.

Several other interesting features can be seen in Fig. 7. There is a relatively wide variation in  $\Sigma$  for the different silicides, particularly for the Co silicides. It is this property that allows each phase to be very easily distinguished in the RPS spectra. There is a correspondingly large variation in  $\phi^+$  with relatively little variation in  $\phi^-$ , as can be seen in Table I. In addition, the value of  $\Sigma$  is surprisingly large compared with that of the pure metal. The Ni silicide peaks all have  $\Sigma$  equal to, or greater than, that of pure Ni even though they rank in order of increasing  $\Sigma$  from Si rich to Ni rich. Naively, one might have expected (on the basis of alloying results<sup>11</sup>) that the silicides would lie between Si and Ni in Fig. 7, with the Ni-rich phase approaching Ni from the left. This is clearly not the case, and thus it would be interesting to have detailed calculations of  $\mu^-$  and  $\mu^+$  for the silicides (as per Ref. 12 for the elements). Another interesting feature is the difference in the ordering of the  $\Sigma$  values for the Co silicides as opposed to the Ni silicides. This may be explained by the fact that while both metal-rich phases have the PbCl<sub>2</sub> structure, and both Si-rich phases have the CaF<sub>2</sub> structure, the structures of the intermediate phases are different; NiSi has the orthorhombic MnP structure, whereas CoSi has the cubic FeSi structure.<sup>18</sup> As a result, the atomic density of CoSi is slightly larger than that of NiSi, which may account for the fact that its  $\Sigma$  value is larger (i.e., less negative) than that of the other silicides. Nonetheless, we were surprised to find such a large value of  $\Sigma$  (−1.85 eV), and such a large and negative  $\phi^+$  (−3.02 eV) for CoSi, comparable to such extreme

TABLE I. Summary of the measured values of the parameter  $\Sigma$ , and the positron and electron work functions  $\phi^+$  and  $\phi^-$ , respectively. All values are in eV. For a discussion of the relative and absolute uncertainties in these quantities refer to Sec. II.

	$\Sigma$	$\phi^+$	$\phi^-$
Co <sub>2</sub> Si <sup>a</sup>	−2.30		
CoSi <sup>a</sup>	−1.85	−3.02	4.87
CoSi <sub>2</sub> <sup>b</sup>	−3.95	−0.60	4.55
NiSi <sup>c</sup>	−3.42	−1.14	4.56
NiSi <sub>2</sub> <sup>c</sup>	−3.70	−0.94	4.64
Ni <sub>2</sub> Si <sup>d</sup>	−2.73	−2.06	4.79
NiSi <sup>d</sup>	−3.49	−1.44	4.93
NiSi <sub>2</sub> <sup>d</sup>	−3.81	−0.73	4.54

<sup>a</sup>Co film of thickness 100 Å deposited on Si(111) substrate and reacted.

<sup>b</sup>Co film of thickness 200 Å deposited on Si(111) substrate and reacted.

<sup>c</sup>Ni film of thickness approximately 50 Å deposited on Si(111) substrate and reacted.

<sup>d</sup>Ni film of thickness approximately 50 Å deposited on Si(100) substrate and reacted.

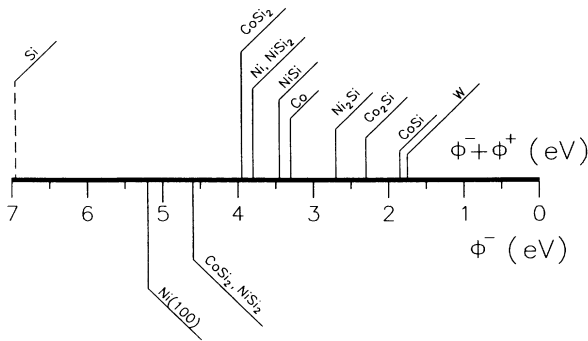


FIG. 7. Measured reemitted-positron elastic peak energies and zero energy cutoffs (the value for Si is a theoretical prediction from Ref. 12). The energy scale is reversed so that positron energy increases to the right. As a result, the upper scale represents  $-\Sigma = \phi^- + \phi^+$ . The lower scale corresponds directly to the electron work functions, which determine the zero energy cutoffs. All peak energies are measured relative to the Ni peak, with the absolute energy scale set by defining  $\phi^-$  for Ni(100) to be 5.2 eV (Ref. 17).

values as those for W.

Another feature that is clearly evident in Figs. 2–4 is that the reemitted-positron yield in the elastic peaks of all of the silicides are small, ranging from approximately 4–20% for the Ni silicides, and approximately 1–10% for the Co silicides, where the yields are given as a fraction of the elastic peak yield of a clean, well-annealed, single-crystal Ni reference. The total (energy-integrated) yield of reemitted positrons shows much less variation, ranging from approximately 15% for the metal-rich and intermediate phases to 25–30% for the Si-rich phase, where the yields are given as a fraction of the total yield of the Ni reference crystal. These results are not surprising for the metal-rich and intermediate phases since the nonepitaxial nature of their growth (indicated by the lack of a LEED pattern) presumably leads to highly defective films. The low peak rates relative to that of the Ni reference indicate that the positrons are emitted with an angular distribution that is much broader than the angular acceptance of our energy analyzer, thus suggesting a rough or faceted surface. The higher reemission rates from the Si-rich phase are certainly due to their better epitaxy. Nevertheless, their relatively low total yields may well be due to the presence of misfit dislocations or other positron-trapping defects, as discussed below.

To further investigate trapping defects in  $\text{CoSi}_2$  films, the total yield of reemitted positrons from a film grown by the deposition of 200 Å of Co and subsequent annealing at 600°C and 850°C are shown in Fig. 8 as a function of incident positron energy. Note that the total yield drops rather sharply with increasing incident energy, and hence implantation depth. The data were fitted to a function of the form<sup>23</sup>  $f = f_0[1 + (E/E_0)^{1.6}]^{-1}$ . The fits yield  $E_0$  values of 1.30 and 1.36 keV for the 600°C and 850°C data, respectively. These low values indicate that the film has a very short positron diffusion length, of order 150 Å. This is in reasonable agreement with the result obtained by Gullikson, Mills, and Phillips for a film grown by

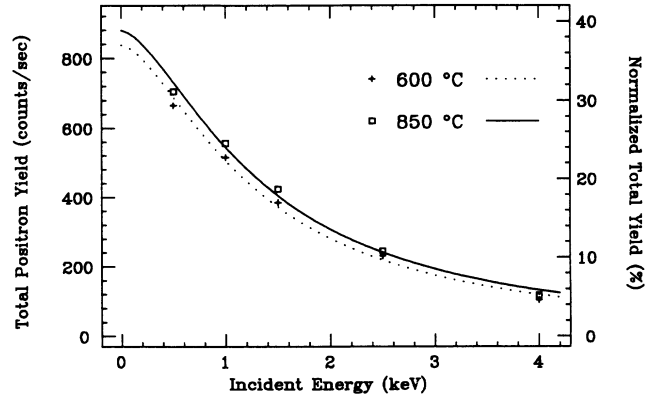


FIG. 8. Total yield at RT of reemitted positrons from a Co film of thickness 200 Å deposited on a Si(111) substrate and annealed at 600°C and 850°C to form  $\text{CoSi}_2$ , as a function of incident positron energy. The right-hand scale represents the total yield as a fraction of the yield (extrapolated to zero incident energy) of a Ni single crystal. The dotted and solid curves represent fits to the 600°C and 850°C data, respectively. The data were fitted to a function of the form  $f = f_0[1 + (E/E_0)^{1.6}]^{-1}$ . The resulting  $E_0$  values are 1.30 and 1.36 keV, respectively.

molecular-beam epitaxy.<sup>10</sup> Note also that the total yield is not significantly increased by annealing at the higher temperature. In the next section we will present evidence that the positron diffusion constant, and hence the diffusion length, in a defect-free crystal of  $\text{CoSi}_2$  should be comparable to that of Ni (several thousand angstroms), and thus the low reemission rate cannot be explained by a small diffusion constant in the bulk silicide. There are either positron-trapping defects (misfit dislocations and/or vacancies) in the film, or the Si interface/Schottky well is trapping most of the positrons in the film. There is evidence for positron-trapping defects, as will be discussed in Sec. VI.

## V. POSITRON DEFORMATION POTENTIAL OF $\text{CoSi}_2$

The positron deformation potential relates changes in  $\Sigma$  to variations in the bulk atomic density,<sup>12</sup> and is defined as  $E_d^+ \equiv V(\partial\Sigma/\partial V)$ . It may be used to estimate the size of the shift in  $\Sigma$  due to volume dilatations caused by strained pseudomorphic growth. The value of the deformation potential may be determined by measuring the shift in  $\Sigma$  due to thermally induced volume dilatations.<sup>24</sup> To this end, the temperature dependence of  $\Sigma$  was measured for several  $\text{CoSi}_2$  films grown by depositing Co films of thickness 100–200 Å on Si(111) substrates and annealing at 850°C. This temperature dependence appears in the RPS spectrum in the form of a shift in the elastic peak energy. The peak energy was measured as a function of temperature as the samples were radiatively heated by a W filament mounted behind the sample. Incident positrons of energy 1 keV were used. As can be seen in Fig. 9, the peak shift was found to be linear in the range from 25 to 275°C, with the slope

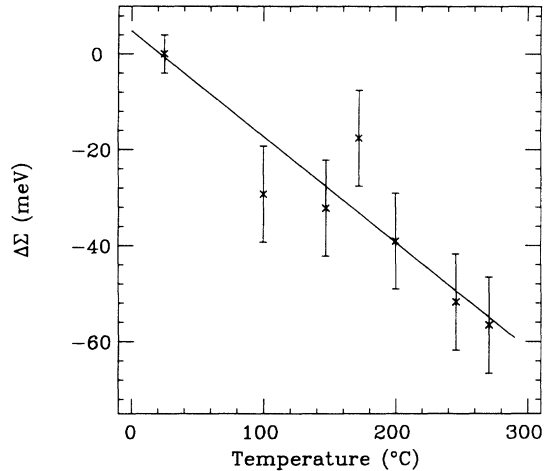


FIG. 9. Shift in  $\text{CoSi}_2$  elastic positron peak energy as a function of sample temperature. The  $\text{CoSi}_2$  films were grown by depositing Co films of thickness 100–200 Å on a Si(111) substrate and annealing at 850°C. RPS spectra were acquired using positrons of incident energy 1 keV. The data are fitted to a line with slope  $d\Sigma/dT = -0.22 \pm 0.03$  meV/K.

$d\Sigma/dT = -0.22 \pm 0.03$  meV/K. This value can be related to  $E_d^+$  using

$$\frac{d\Sigma}{dT} = 3\alpha E_d^+ + \left[ \frac{\partial \Sigma}{\partial T} \right]_V, \quad (2)$$

where  $\alpha$  is the linear coefficient of thermal expansion. The second term,

$$\left[ \frac{\partial \Sigma}{\partial T} \right]_V = \left[ \frac{\partial \mu^-}{\partial T} \right]_V + \left[ \frac{\partial \mu^+}{\partial T} \right]_V, \quad (3)$$

is due to the effects of lattice vibrations. Its relative size is not accurately known, but Herring and Nichols<sup>25</sup> claim that, for most metals,  $(\partial \mu^- / \partial T)_V$  is of order a fraction of  $k_B$  (0.086 meV/K). In addition,  $(\partial \mu^+ / \partial T)_V$  is expected to have the opposite sign,<sup>26</sup> and therefore the positron and electron contributions may to some extent cancel each other in Eq. (3). Under the assumption that  $(\partial \Sigma / \partial T)_V$  may be neglected at the 10% level (i.e., the temperature dependence at the 0.02-meV/K level is due to thermal *volume* expansion), we can use the first term in Eq. (2) to determine  $E_d^+$  (this approximation was found to be justified in the case of Ni).<sup>13</sup> Using  $\alpha = 10.1 \times 10^{-6} \text{ K}^{-1}$ ,<sup>27</sup> the measured temperature dependence then yields  $E_d^+ = -7.3 \pm 1.0$  eV where the error quoted is due to the statistical error in determining  $d\Sigma/dT$ .

The deformation potential is also a measure of the strength of the positron-phonon coupling, and therefore may be used to estimate the size of the positron diffusion constant,  $D^+$ , due to acoustic-phonon scattering.<sup>26</sup> The diffusion constant is directly related to the positron diffusion length,<sup>16</sup> which determines many of the positron transport properties of a material. Using the measured values of the elastic constants,<sup>28</sup> and taking the effective mass of the positron to be  $m^* = 1.5m_e$ , which represents

a reasonable compromise between theoretical and experimental estimates for most materials,<sup>26</sup> the above value of  $E_d^+$  yields the relatively large value of 2.9  $\text{cm}^2/\text{s}$  for  $D^+$  at 300 K [typical metals have diffusion constants of order 0.1–1.0  $\text{cm}^2/\text{s}$  (Ref. 16)]. In the absence of positron-trapping defects, the resulting positron diffusion length is of order several thousand angstroms, comparable to that of Ni. Thus the relatively low yield of reemitted positrons from the silicides indicates that a significant number of positrons are trapping. We will consider this point further in the following section.

## VI. ULTRATHIN $\text{CoSi}_2$ FILMS

As mentioned earlier, strained pseudomorphic growth leads to volume dilatations which should appear in RPS as shifts in the elastic peak energy. The growth of pseudomorphic  $\text{CoSi}_2$  films by the reaction of Co deposited on Si(111) substrates at room temperature has been reported, with a critical thickness of approximately 30–40 Å.<sup>5</sup> X-ray studies have indicated that above this thickness the films may still be significantly strained, with the strain gradually relaxing as the film thickness increases to several hundred angstroms.<sup>29,30</sup>

The volume dilatation of pseudomorphically strained films may be calculated using the measured values of the elastic constants<sup>28</sup> of  $\text{CoSi}_2$ . Equal strains of 1.2% in the surface plane result in a calculated volume increase of 1.42% for the pseudomorphic film. Using our measured value of the deformation potential, the peak shift is estimated to be approximately  $-105$  meV (a shift to the left in Fig. 7). Such a shift should be readily resolved. In an attempt to observe these shifts,  $\text{CoSi}_2$  films as thin as 15 Å were grown on Si(111) substrates. Co films were deposited with deposition rates of order 0.2 Å/s and annealed at either 600°C or 850°C to form  $\text{CoSi}_2$  films. Some films were grown by a single deposition and anneal, others by multiple deposition and annealing steps. The background pressure in the chamber remained below  $2 \times 10^{-9}$  Torr at all times during the deposition and annealing. No shift as large as 105 meV was observed. All films of thickness less than or equal to the nominal critical thickness had broadened, asymmetric peaks that were shifted to higher positron energy (a shift to the right in Fig. 7) by as much as 50 meV. This is almost certainly due to the inability of positrons with a mean free path of order 30 Å (Ref. 11) to thermalize in a film of comparable thickness. The broadening of the peak and its shift toward higher energy is due to a large tail of nonthermal positrons that effectively renders the pseudomorphic peak shift unobservable. For films of thickness greater than 40 Å the peaks become narrower and more symmetric, due to a decrease in the number of nonthermals emitted. The film thickness required to fully thermalize a significant number of positrons apparently exceeds the critical thickness for fully strained pseudomorphic growth. For some films of thickness 50–100 Å we observed peak shifts as large as  $-50$  meV. These shifts are interpreted as being due to residual strain in partially relaxed films. The peak positions of thick films (starting Co thickness 150–200 Å) give no indication (at the  $\pm 20$ -meV

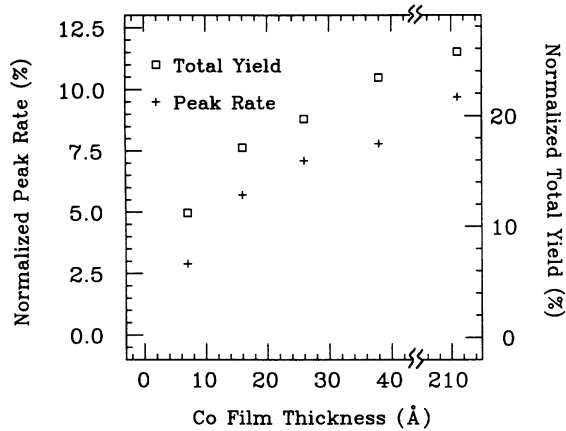


FIG. 10. Elastic positron peak rate and total yield of reemitted positrons at RT, as a fraction of that of a Ni single crystal, for  $\text{CoSi}_2$  films grown on a Si(111) substrate. The films were grown by sequential steps of Co deposition followed by annealing at  $850^\circ\text{C}$ . All data were acquired using positrons of incident energy 1 keV (mean implantation depth approximately  $80 \text{ \AA}$ ).

level) of any residual strain.

As mentioned earlier, all of the silicides exhibit relatively small reemitted-positron yields. We concluded in Sec. IV that in all likelihood the metal-rich and intermediate phases have a high density of open-volume defects that trap positrons, but that the situation for the Si-rich phase was less clear. In order to distinguish trapping in bulk defects from trapping at the Si interface/Schottky well, we measured the positron peak rate and total yield of ultrathin  $\text{CoSi}_2$  films that were grown by a multiple-step deposition and  $850^\circ\text{C}$  reaction technique. These data (acquired using 1-keV incident positrons with  $\bar{z} \approx 80 \text{ \AA}$ ) are plotted in Fig. 10, as a function of the initial Co film thickness. We find that both the peak rate and total yield approach the thick film ( $700\text{-\AA}$ ) values of 8–10% and 25–30%, respectively, for a Co film thickness of order  $40 \text{ \AA}$  (corresponding to  $140\text{-\AA}$   $\text{CoSi}_2$  thickness). This is consistent with a *bulk* diffusion length of order  $150 \text{ \AA}$  (in agreement with our depth-profiling results). It is not consistent with a long *bulk* diffusion length (e.g., no bulk defects) and trapping only at the interface. If this were the case, a sizable increase in reemission (of order 50%) would be expected when the film thickness is increased from  $140$  to  $700 \text{ \AA}$ . Thus the Si interface/Schottky well is not the major source of positron trapping, and we therefore conclude that the positrons are mainly trapping in misfit dislocations/and or vacancies.

## VII. CONCLUSION

All of the different phases of Co and Ni silicides reemit positrons, with  $\phi^+$  ranging from  $-0.6$  to  $-3.0 \text{ eV}$ . As there is little variation in  $\phi^-$ , the parameter  $\Sigma$  (which

represents the positron energy level in a particular material) therefore also has a comparably large variation. In general,  $\Sigma$  increases with increasing atomic density, which in turn tends to decrease with the silicide reaction temperature as the film is transformed from the metal-rich to the Si-rich phase. The rate of positron reemission in the elastic peak increases in going from the metal-rich to the Si-rich phase. This feature, together with the widely separated and thus easily distinguishable peaks in the RPS spectra for each silicide phase, should provide the necessary image contrast for observing each phase on a microscopic scale using the positron reemission microscope (PRM).<sup>31,32</sup> Depth-profiled PRM images may provide a unique perspective on the dynamics of the silicide growth as it proceeds through the various phases by diffusion and/or nucleation. In the particular case of  $\text{CoSi}_2$  films, a PRM with the predicted lateral resolution of order  $10 \text{ \AA}$  (Refs. 31 and 32) could readily be used to observe the formation of nonemitting Si pinholes, which have lateral dimensions larger than  $100 \text{ \AA}$ .<sup>4</sup> Such pinholes play a strong role in determining the electron transport properties of Si/ $\text{CoSi}_2$ /Si metal and permeable base transistors.<sup>2,3</sup>

Our measurement of the positron deformation potential leads us to expect a shift in  $\Sigma$  of order  $-105 \text{ meV}$  for strained pseudomorphic  $\text{CoSi}_2$  films. However, RPS does not appear to be sensitive to such shifts, since films of thickness less than  $40 \text{ \AA}$  have broad RPS peaks with shifts of the opposite sign, due to incomplete thermalization of the positrons in such thin films. Nonetheless, the measured deformation potential can be used, along with a reasonable estimate of the positron effective mass, to deduce that the positron diffusion constant in  $\text{CoSi}_2$  is comparable to that of typical metals. Thus the short positron diffusion length (of order  $150 \text{ \AA}$ ) determined in depth-profiling measurements cannot be attributed to a small diffusion constant. Positrons must be trapping in the Schottky well, or in defects in the film, or at the interface with Si substrate. Our RPS measurements, considered as a function of film thickness, distinguish defects in the film (presumably misfit dislocations and/or vacancies) as the dominant source of positron trapping. We cannot distinguish any significant trapping at the Si interface/Schottky well. It would be interesting to employ depth-profiled Doppler broadening spectroscopy<sup>16</sup> on a thick  $\text{CoSi}_2$  film to provide further confirmation of this conclusion.

## ACKNOWLEDGMENTS

We thank S. M. Yalisove, and members of the Michigan positron group for helpful discussions. We also thank F. L. Terry for providing the Si substrates. This work was supported by the National Science Foundation, Grant No. DMR-9 003 987, with some shared equipment assistance from Grant No. PHY-9 119 899.

- <sup>1</sup>R. T. Tung and J. M. Gibson, in *Heteroepitaxy on Silicon*, edited by J. C. C. Fan and J. M. Poate, MRS Symposia Proceedings No. 67 (Materials Research Society, Pittsburgh, 1986), p. 211.
- <sup>2</sup>A. F. J. Levi, R. T. Tung, J. L. Batstone, and M. Anzlowar, in *Epitaxy of Semiconductor Layered Structures*, edited by R. T. Tung, L. R. Dawson, and R. L. Gunshor, MRS Symposia Proceedings No. 102 (Materials Research Society, Pittsburgh, 1988), p. 361.
- <sup>3</sup>R. T. Tung, A. F. J. Levi, and J. M. Gibson, *Appl. Phys. Lett.* **48**, 635 (1986).
- <sup>4</sup>R. T. Tung, in *Silicon-Molecular Beam Epitaxy*, Vol. II, edited by E. Kasper and J. C. Bean (CRC, Boca Raton, 1988).
- <sup>5</sup>J. L. Batstone, J. M. Phillips, and J. M. Gibson, in *Heteroepitaxy on Silicon II*, edited by J. C. C. Fan, J. M. Phillips, and B.-Y. Tsaur, MRS Symposia Proceedings No. 91 (Materials Research Society, Pittsburgh, 1987), p. 445.
- <sup>6</sup>J. L. Batstone, R. T. Tung, J. M. Phillips, and J. M. Gibson, in *Epitaxy of Semiconductor Layered Structures*, edited by R. T. Tung, L. R. Dawson, and R. L. Gunshor, MRS Symposia Proceedings No. 102 (Materials Research Society, Pittsburgh, 1988), p. 253.
- <sup>7</sup>K. G. Lynn and B. T. A. McKee, *Appl. Phys.* **19**, 247 (1979).
- <sup>8</sup>C. D. Beling *et al.*, *Appl. Phys. A* **42**, 111 (1987).
- <sup>9</sup>T. C. Leung *et al.*, *Appl. Phys. Lett.* **58**, 86 (1991).
- <sup>10</sup>E. M. Gullikson, A. P. Mills, Jr., and J. M. Phillips, *Surf. Sci.* **195**, L150 (1988).
- <sup>11</sup>D. W. Gidley and W. E. Frieze, *Phys. Rev. Lett.* **60**, 1193 (1988).
- <sup>12</sup>M. J. Puska, P. Lanki, and R. M. Nieminen, *J. Phys. Condens. Matter* **1**, 6081 (1989).
- <sup>13</sup>D. W. Gidley, *Phys. Rev. Lett.* **62**, 811 (1989).
- <sup>14</sup>W. E. Frieze, D. W. Gidley, and B. D. Wissman, *Solid State Commun.* **74**, 1079 (1990).
- <sup>15</sup>K. N. Tu and J. W. Mayer, in *Thin Films—Interdiffusion and Reactions*, edited by J. M. Poate, K. N. Tu, and J. W. Mayer (Wiley, New York, 1978).
- <sup>16</sup>P. J. Schultz and K. G. Lynn, *Rev. Mod. Phys.* **60**, 701 (1988).
- <sup>17</sup>B. G. Baker, B. B. Johnson, and G. L. C. Maire, *Surf. Sci.* **24**, 572 (1971).
- <sup>18</sup>M.-A. Nicolet and S. S. Lau, in *VLSI Electronics: Microstructure Science*, edited by N. G. Einspruch and G. B. Larrabee (Academic, New York, 1983), Vol. 6.
- <sup>19</sup>C.-D. Lien, M.-A. Nicolet, C. S. Pai, and S. S. Lau, *Appl. Phys. A* **36**, 153 (1985).
- <sup>20</sup>C. d'Anterrosches, *Surf. Sci.* **168**, 751 (1986).
- <sup>21</sup>F. d'Heurle, S. Petersson, L. Stolt, and B. Strizker, *J. Appl. Phys.* **53**, 5678 (1982).
- <sup>22</sup>F. M. d'Heurle and P. Gas, *J. Mater. Res.* **1**, 205 (1986).
- <sup>23</sup>B. Nielsen, K. G. Lynn, A. Vehanen, and P. J. Schultz, *Phys. Rev. B* **32**, 2296 (1985).
- <sup>24</sup>E. M. Gullikson and A. P. Mills, Jr., *Phys. Rev. B* **35**, 8759 (1987).
- <sup>25</sup>C. Herring and M. H. Nichols, *Rev. Mod. Phys.* **21**, 185 (1949).
- <sup>26</sup>O. V. Boev, M. J. Puska, and R. M. Nieminen, *Phys. Rev. B* **36**, 7786 (1987).
- <sup>27</sup>C. W. T. Bulle-Lieuwma, A. H. Van Ommen, and J. Hornstra, in *Epitaxy of Semiconductor Layered Structures*, edited by R. T. Tung, L. R. Dawson, and R. L. Gunshor, MRS Symposia Proceedings No. 102 (Materials Research Society, Pittsburgh, 1988), p. 377.
- <sup>28</sup>G. Guénin, M. Ignat, and O. Thomas, *J. Appl. Phys.* **68**, 6515 (1990).
- <sup>29</sup>K. L. Wang and Y. C. Kao, in *Heteroepitaxy on Silicon* (Ref. 1), p. 235.
- <sup>30</sup>D. N. Jamieson *et al.*, in *Heteroepitaxy on Silicon II* (Ref. 5), p. 429.
- <sup>31</sup>J. Van House and A. Rich, *Phys. Rev. Lett.* **61**, 488 (1988).
- <sup>32</sup>G. R. Brandes, K. F. Canter, and A. P. Mills, Jr., *Phys. Rev. Lett.* **61**, 492 (1988).